


Comparison of iterative model, hybrid iterative, and filtered back projection reconstruction techniques in low-dose brain CT: impact of thin-slice imaging

Takeshi Nakaura^{1,2}  · Yuji Iyama^{1,2} · Masafumi Kidoh^{1,2} · Koichi Yokoyama^{1,2} · Seitaro Oda² · Shinichi Tokuyasu³ · Kazunori Harada⁴ · Yasuyuki Yamashita²

Received: 27 September 2015 / Accepted: 7 December 2015 / Published online: 29 December 2015
© Springer-Verlag Berlin Heidelberg 2015

Abstract

Introduction The purpose of this study was to evaluate the utility of iterative model reconstruction (IMR) in brain CT especially with thin-slice images.

Methods This prospective study received institutional review board approval, and prior informed consent to participate was obtained from all patients. We enrolled 34 patients who underwent brain CT and reconstructed axial images with filtered back projection (FBP), hybrid iterative reconstruction (HIR) and IMR with 1 and 5 mm slice thicknesses. The CT number, image noise, contrast, and contrast noise ratio (CNR) between the thalamus and internal capsule, and the rate of increase of image noise in 1 and 5 mm thickness images between the reconstruction methods, were assessed. Two independent radiologists assessed image contrast, image noise, image sharpness, and overall image quality on a 4-point scale. **Results** The CNRs in 1 and 5 mm slice thickness were significantly higher with IMR (1.2 ± 0.6 and 2.2 ± 0.8 , respectively) than with FBP (0.4 ± 0.3 and 1.0 ± 0.4 , respectively) and HIR (0.5 ± 0.3 and 1.2 ± 0.4 , respectively) ($p < 0.01$). The mean rate of increasing noise from 5 to 1 mm thickness images was significantly lower with IMR (1.7 ± 0.3) than with FBP (2.3 ± 0.3) and HIR (2.3 ± 0.4) ($p < 0.01$). There were no significant

differences in qualitative analysis of unfamiliar image texture between the reconstruction techniques.

Conclusion IMR offers significant noise reduction and higher contrast and CNR in brain CT, especially for thin-slice images, when compared to FBP and HIR.

Keywords CT · Iterative reconstruction · Brain · Radiation dose

Introduction

Dose reduction in computed tomography (CT) has become of major importance due to concerns over the risks of carcinogenesis related to ionizing radiation [1–3]. Nevertheless, dose reduction must be balanced by an acceptable level of image quality, and diagnostic accuracy must be adequately maintained. Image noise is a particularly serious problem for brain CT, as the safe level of CT imaging in normal brain tissues such as the gray and white matter regions is as low as 5–10 Hounsfield unit (HU) [4, 5]. As such, brain CT is traditionally reconstructed with a relatively thick image slice thickness (5 mm for the new multislice CT and 10 mm for the older CT), as image noise is inversely proportional to the square root of the slice thickness [6]. However, it was previously suggested that the thick reconstruction slices are prone to partial volume effects that can interfere with assessment of small hemorrhage [7]. Additionally, CT scanners generally minimize the beam-hardening effect of the cranial bone by using calibration correction and iterative beam-hardening correction software. However, these techniques can often over- or under-correct due to complicated patient anatomy [8]. Therefore, obtaining high spatial resolution brain CT with adequate image noise is difficult without increasing the radiation dose.

✉ Takeshi Nakaura
kff00712@nifty.com

¹ Diagnostic Radiology, Amakusa Medical Center, Kameba 854-1, Amakusa, Kumamoto 863-0046, Japan

² Department of Diagnostic Radiology, Graduate School of Medical Sciences, Kumamoto University, Kumamoto, Japan

³ Philips Electronics, Kumamoto, Japan

⁴ Department of Surgery, Amakusa Medical Center, Kumamoto, Japan

Table 1 Scan parameters of brain CT

| Scan parameters | |
|---------------------------|-------------|
| Beam collimation (mm) | 128 × 0.625 |
| Slice thickness (mm) | 5, 1 |
| Tube voltage (kVp) | 120 |
| Tube current (mA) | 293 |
| Rotation time (s) | 0.4 |
| CTDI _{vol} (mGy) | 40.8 |

CTDI_{vol} volume CT dose index

An iterative reconstruction (IR) algorithm for CT was previously introduced to reduce the image noise, and recent studies suggest that iterative reconstruction techniques are suitable for low-dose brain CT [9, 10]. However, these studies also recommended that such IR techniques must be used with low noise reduction settings due to the appearance of unfamiliar image texture and blocky noise when compared with the filtered back projection (FBP) technique [9]. Nevertheless, the recent evolution of the IR technique may allow development of a full-IR system with more sophisticated modeling of the real CT system, with promising results reported for various CT examinations [11–15]. However, these reconstruction techniques have only one reconstruction parameter and are not specialized to brain CT examination. Further, to our knowledge, clinical studies evaluating the utility of a full-IR technique with a system model for brain CT are unavailable.

The iterative model reconstruction algorithm is a full-IR technique that includes statistical and physical/system models with specialized reconstruction parameters for various imaging methods including brain CT. In the present study, we used this system to evaluate the utility of IMR in brain CT, particularly with thin-slice images.

Materials and methods

This prospective study received institutional review board approval. Prior informed consent to participate was obtained from all patients.

Patients

Between February and March 2014, 34 patients with a suspicion or a past history of brain disease were enrolled in this study. There were 18 males and 16 females, ranging in age from 16 to 94 years (mean 66.7 years).

CT scanning and reconstruction

All patients were scanned on a 256-slice MDCT scanner (Brilliance iCT, Philips Healthcare, Cleveland, OH, USA) with 120 kVp, a 0.4 s gantry rotation, helical pitch of 0.39, and a 293 mA tube current. The detailed scan parameters are shown in Table 1. For an estimation of the CT radiation dose, the CT volume dose index (CTDI_{vol}) and the dose length product (DLP) were recorded. The effective dose (ED) for brain CT was derived from the product of DLP and a conversion coefficient for the brain, as previously reported ($k=0.0021 \text{ mSv mGy}^{-1} \text{ cm}^{-1}$) [16].

Image reconstruction was performed in a 25-cm display field of view (FOV) with 1 and 5 mm slice thicknesses. All images were reconstructed using a standard (FBP) algorithm with a standard brain kernel (UB), the hybrid iterative reconstruction with a standard brain kernel (UB, iDose⁴—level 2), and the IMR technique (IMR—neuro routine level 1). We selected low iterative reconstruction levels (hybrid iterative

Table 2 Quantitative image analysis

| | Thickness | FBP | HIR | IMR | <i>p</i> Value (pairwise comparisons) | | |
|--------------------------------------|-----------|------------|------------|------------|---------------------------------------|------------|------------|
| | | | | | FBP vs HIR | FBP vs IMR | HIR vs IMR |
| Mean CT number—thalamus (HU) | 1 mm | 31.3 ± 2.3 | 31.3 ± 2.2 | 30.6 ± 2.1 | 0.91 | <0.01 | <0.01 |
| Mean CT number—internal capsule (HU) | | 26.7 ± 2.1 | 26.7 ± 2.0 | 25.9 ± 1.5 | 0.90 | <0.01 | <0.01 |
| Contrast (HU) | | 4.5 ± 2.7 | 4.5 ± 2.6 | 4.7 ± 1.9 | 0.98 | 0.36 | 0.52 |
| Image noise (HU) | | 11.3 ± 1.7 | 9.5 ± 1.5 | 4.0 ± 0.7 | <0.01 | <0.01 | <0.01 |
| CNR | | 0.4 ± 0.3 | 0.5 ± 0.3 | 1.2 ± 0.6 | <0.01 | <0.01 | <0.01 |
| Mean CT number—thalamus (HU) | 5 mm | 31.4 ± 1.8 | 31.4 ± 1.8 | 30.6 ± 1.8 | 1.00 | <0.01 | <0.01 |
| Mean CT number—internal capsule (HU) | | 26.6 ± 1.5 | 26.6 ± 1.5 | 25.5 ± 1.4 | 0.73 | <0.01 | <0.01 |
| Contrast (HU) | | 4.9 ± 1.7 | 4.8 ± 1.7 | 5.1 ± 1.6 | 0.71 | <0.01 | <0.01 |
| Image noise (HU) | | 4.9 ± 0.5 | 4.1 ± 0.4 | 2.4 ± 0.3 | <0.01 | <0.01 | <0.01 |
| CNR | | 1.0 ± 0.4 | 1.2 ± 0.4 | 2.2 ± 0.8 | <0.01 | <0.01 | <0.01 |
| Noise increasing rate | — | 2.3 ± 0.3 | 2.3 ± 0.4 | 1.7 ± 0.3 | 0.79 | <0.01 | <0.01 |

Data are shown as the mean ± standard deviation

FBP filtered back projection, HIR hybrid iterative reconstruction, IMR iterative model reconstruction, CNR contrast noise ratio

level of 2 and an IMR level of 1) for this study because previous reports suggested that the high level iterative reconstruction cannot preserve the low contrast detectability [17–19] and the vander recommended us to use the low level iterative reconstruction for brain imaging.

Quantitative image analysis

A board-certified radiologist with 19-year experience with brain CT performed quantitative image analysis on 1 and 5 mm thickness images with each reconstruction technique. The mean attenuation of the thalamus ($CT\#_{\text{thalamus}}$) without pathology in a circular region of interest (ROI) of 10 mm and the internal capsule ($CT\#_{\text{internal capsule}}$) without pathology in a circular ROI of 4 mm were measured. In addition, to evaluate the image noise, we measured the standard deviation (SD) of attenuation on the ROI of the thalamus. To minimize bias from single measurements, we measured three ROIs in three different sequential slices for all ROIs and calculated the mean of all measurements. Image noise was defined as the SD of ROI of the thalamus. The CNR was calculated as follows:

$$\text{CNR} = (CT\#_{\text{thalamus}} - CT\#_{\text{internal capsule}}) / (\text{image noise})$$

We also calculated the noise increasing rate (NIR) of hybrid iterative reconstruction (HIR) and IMR to FBP from the 1 to 5 mm thickness images as follows:

$$\text{NIR} = (\text{image noise of 1 mm thickness images}) / (\text{image noise of 5 mm thickness images}).$$

Qualitative image analysis

To evaluate the image quality under the different protocols, we performed qualitative image analysis at a window level of 40 HU and a width of 100 HU (standard brain window setting) on a PACS viewer (Synapse; Fuji Film Medical). Two board-certified radiologists with 5 and 8 years of respective experience with brain CT independently graded image contrast, image noise, image sharpness, image texture, and overall image quality. The CT datasets were randomized, and the radiologists were blinded to the acquisition parameters; they were allowed to adjust the window level and width. Using a 4-point subjective scale, they independently graded image contrast and overall image quality (1 = unacceptable, 2 = acceptable, 3 = good, 4 = excellent). Image noise and unfamiliar image texture were similarly graded as image noise or unfamiliar image texture present and unacceptable = grade 1, image noise or unfamiliar image texture present and interfering with the depiction of adjacent structures = grade 2, image noise or unfamiliar image texture present without interfering with the depiction of adjacent structures = grade 3, and no noise or unfamiliar image

texture = grade 4. Image sharpness was graded by evaluating the brain surface sharpness as blurry = grade 1, poorer than average = grade 2, better than average = grade 3, and sharpest = grade 4. In cases of interobserver disagreement, final decisions were reached by consensus.

Statistical analysis

All numeric values are reported as the mean \pm SD. The CT numbers, contrast, image noise, and CNR of each of the reconstruction images were compared using the Kruskal-Wallis test. If there was a statistically significant difference among the different reconstruction techniques, we performed pairwise comparisons with the Holm test. For qualitative analysis, we used the Friedman's test and the Scheffe's test.

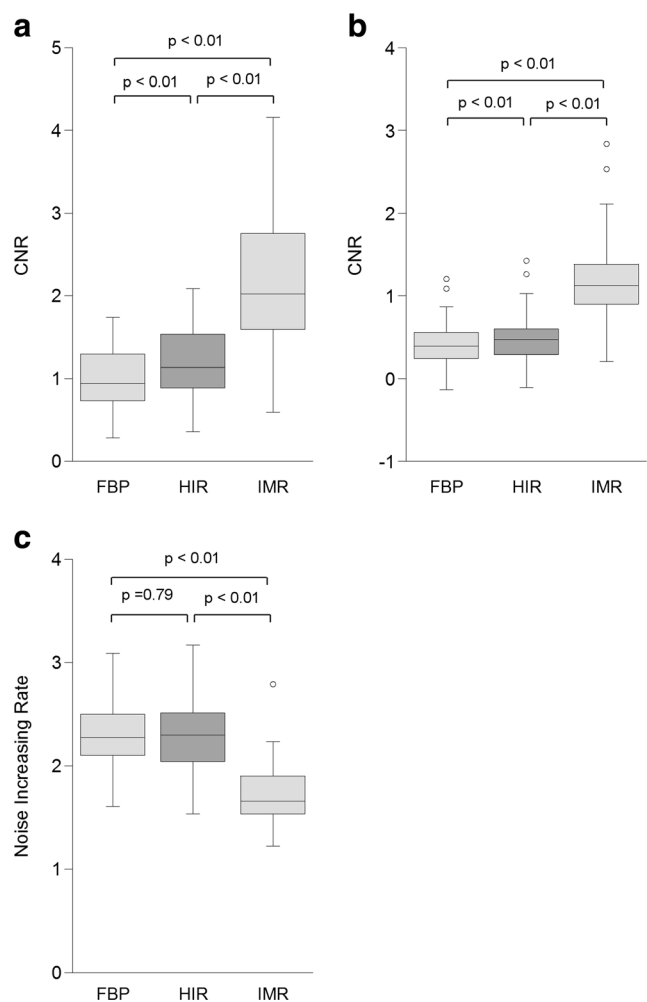


Fig. 1 Quantitative image analysis of the contrast noise ratio and the noise increasing rate with 1-mm-thick images. The contrast noise ratio of the iterative model reconstruction was significantly higher than the hybrid iterative reconstruction and the filtered back projection with 5-mm slice thickness images (a) and with 1-mm slice thickness images (b) ($p < 0.01$). The mean noise increasing rate from 5 to 1-mm-thick images was significantly lower with iterative model reconstruction than that with the other reconstruction techniques ($p < 0.01$)

Table 3 Results of qualitative image analysis

| | FBP | HIR | IMR | Kappa | <i>p</i> Value (pairwise comparisons) | | |
|--------------------------|-----------|-----------|-----------|-------|---------------------------------------|------------|------------|
| | | | | | FBP vs HIR | FBP vs IMR | HIR vs IMR |
| Image contrast | 3.1 ± 0.7 | 3.5 ± 0.6 | 3.8 ± 0.4 | 0.63 | 0.60 | 0.01 | 0.26 |
| Image noise | 1.9 ± 0.8 | 2.5 ± 0.7 | 3.6 ± 0.5 | 0.66 | 0.25 | <0.01 | 0.01 |
| Image sharpness | 2.1 ± 0.5 | 2.7 ± 0.7 | 3.6 ± 0.5 | 0.45 | 0.18 | <0.01 | 0.04 |
| Unfamiliar image texture | 3.6 ± 0.5 | 3.4 ± 0.5 | 3.5 ± 0.5 | 0.54 | 0.58 | 0.91 | 0.93 |
| Overall image quality | 2.0 ± 0.7 | 2.8 ± 0.8 | 3.6 ± 0.5 | 0.64 | 0.08 | <0.01 | 0.10 |

Data are shown as the mean ± standard deviation

FBP filtered back projection, HIR hybrid iterative reconstruction, IMR iterative model reconstruction

Differences of $p < 0.05$ were considered statistically significant. The scale for the Kappa coefficients for interobserver agreement was less than 0.20 = poor, 0.21–0.40 = fair, 0.41–0.60 = moderate, 0.61–0.80 = substantial, and 0.81–1.00 = near perfect. Statistical analyses were performed with the free statistical software “R” (R, version 2.6.1; The R Project for Statistical Computing; <http://www.r-project.org/>).

Results

Quantitative image analysis

The results of the quantitative image analysis of patients are summarized in Table 2 and Fig. 1. The average DLP and the ED were 833.5 ± 67.1 mGy cm and 1.75 ± 0.01 mSv, respectively. The mean CT numbers of the thalamus and the internal capsule were significantly lower with IMR images than with FBP and HIR in 1 and 5 mm thickness images ($p < 0.01$). The

contrast of the thalamus and the internal capsule was significantly higher with IMR (5.1 ± 0.2 HU) than with FBP (4.9 ± 1.7 HU) and HIR (4.8 ± 1.7 HU) in 5 mm thickness images ($p < 0.01$). The image noise was significantly lower with IMR (1 mm 4.0 ± 0.7 HU, 5 mm 2.4 ± 0.3 HU) compared to FBP (1 mm 11.3 ± 1.7 HU, 5 mm 4.9 ± 0.5 HU) and HIR (1 mm 9.5 ± 1.5 HU, 5 mm 4.1 ± 0.4 HU) ($p < 0.01$). The CNR in 1 and 5 mm slice thickness images were significantly higher with IMR (1.2 ± 0.6 and 2.2 ± 0.8 , respectively) than with FBP (0.4 ± 0.3 and 1.0 ± 0.4 , respectively) and HIR (0.5 ± 0.3 and 1.2 ± 0.4 , respectively) ($p < 0.01$). The mean noise increasing rate from 5 to 1 mm thickness images was significantly lower with IMR (1.7 ± 0.3) than that with FBP (2.3 ± 0.3) and HIR (2.3 ± 0.4) ($p < 0.01$).

Qualitative image analysis

On visual evaluation, there were no significant overall differences in unfamiliar image texture. However, there were

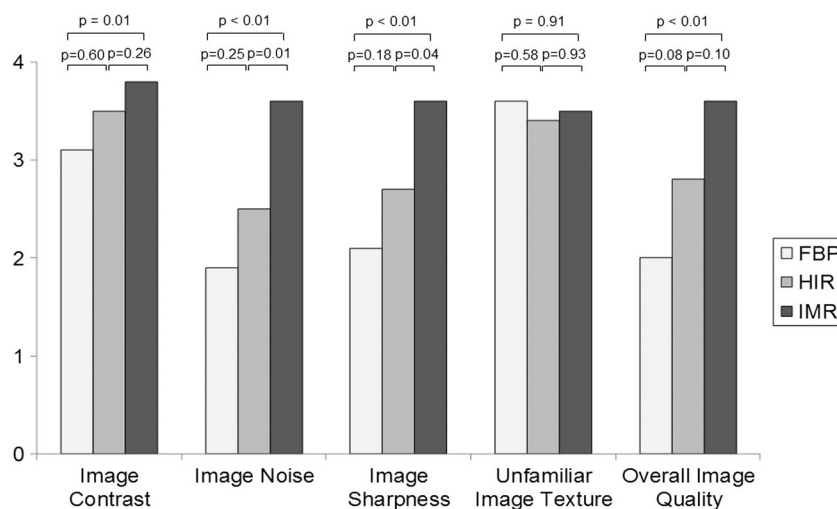


Fig. 2 Qualitative image analysis. Pairwise comparisons revealed that iterative model reconstruction provided significantly higher scores in image contrast, image noise, image sharpness, image texture, and overall image quality than filtered back projection ($p < 0.05$). The iterative model reconstruction also provided significantly higher scores

in image noise, image sharpness, and overall image quality than hybrid iterative reconstruction ($p < 0.05$). However, there were no differences in all qualitative analysis between filtered back projection and hybrid iterative reconstruction

significant overall differences with respect to image noise, image sharpness, and overall image quality ($p < 0.05$) (Table 3, Fig. 2). Pairwise comparisons revealed that IMR provided significantly higher scores in image contrast, image noise, image sharpness, image texture and overall image quality than FBP ($p < 0.05$). IMR also provided significantly higher scores in image noise, image sharpness and overall image quality than HIR ($p < 0.05$). However, there were no significant differences in all qualitative analyses between FBP and HIR. There was moderate-to-substantial interobserver agreement for image contrast, image noise, image sharpness, image texture, and overall image quality (kappa=0.63, 0.66, 0.45, 0.54, and 0.64, respectively). Representative cases are shown in Figs. 3 and 4.

Discussion

Our results demonstrate that the IMR technique significantly improved both qualitative and quantitative image quality in low-dose brain CT when compared with the FBP and HIR techniques. This advanced IR technique offers extremely higher noise reduction, especially in thin-slice images, than

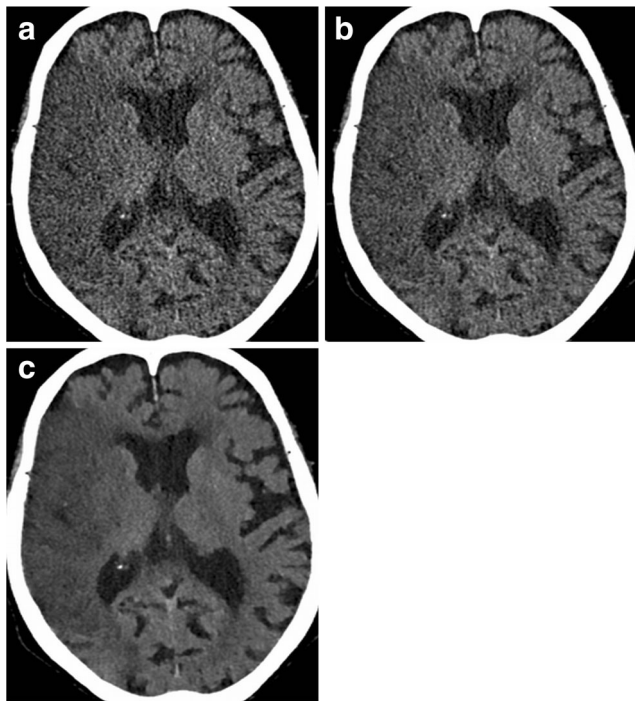


Fig. 3 Thin-slice thickness (1 mm) transverse images and the multiplanar reformation images of filtered back projection (a), hybrid iterative reconstruction (b), and iterative model reconstruction (c) for an 87-year-old man with acute right middle cerebral artery thrombosis. The iterative model reconstruction provided significant noise reduction compared with hybrid iterative reconstruction and filtered back projection and clearly depicted the border of the infarction area. The iterative model reconstruction also increased the contrast between the cerebral infarction area and the non-infarction area

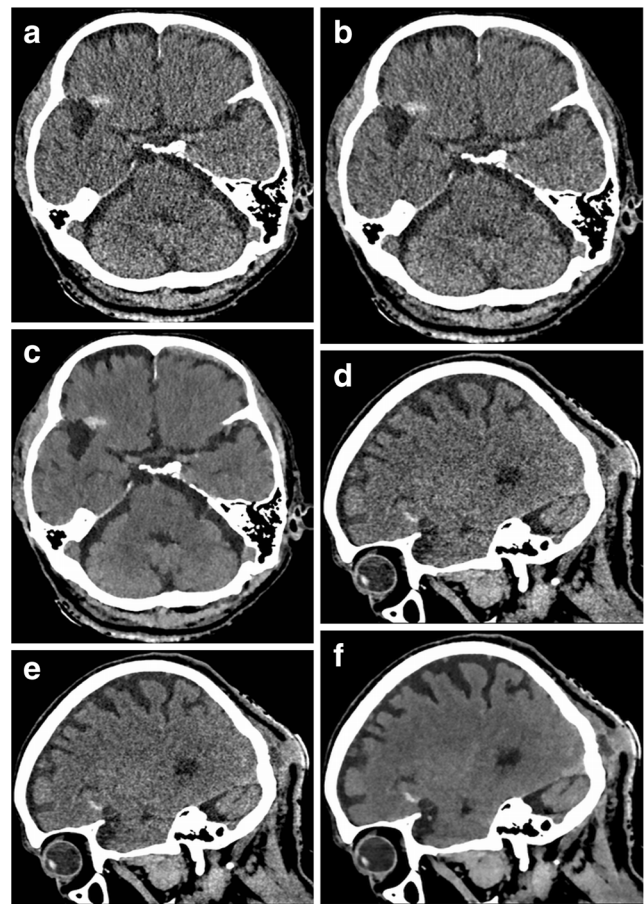


Fig. 4 Thin-slice thickness (1 mm) transverse images and the multiplanar reformation images of filtered back projection (a, d), hybrid iterative reconstruction (b, e), and iterative model reconstruction (c, f) for brain CT in a 71-year-old man with a traffic accident. Thin-slice thickness (1 mm) transverse images with iterative model reconstruction clearly depicted the small brain contusion in the right frontal lobe, and the image noise was lower than other reconstruction techniques

that with the HIR technique. Additionally, unfamiliar image texture was not a significant problem for the IMR technique.

Many studies have suggested that the full-IR method is suitable for the majority of imaging modalities. However, it has not been widely applied to brain CT, and compared with other techniques, image reconstruction of brain CT requires assessment of the beam-hardening effect from the skull bone, which may lead to artifacts if not correctly handled during reconstruction. In FBP-based methods, the beam hardening due to bone is generally corrected by post-processing steps [20]. For example, the initial images are first reconstructed using uncorrected projection data. Secondly, the bone is detected using a Hounsfield unit cutoff. Thirdly, these are forward projected and a custom beam-hardening correction for each detector element is performed. Lastly, the final images are reconstructed using corrected projection data. For full-IR methods, a number of methods have been introduced into the iterative reconstruction loop or directly on the projection data to avoid beam-hardening artifacts [21]. However, this process

can make it difficult to develop a full-IR method for the brain when compared with other examinations.

Our data suggests that IMR provides a higher image noise reduction than that for HIR especially with thin-slice images. The reason why IMR can reduce more image noise than HIR might be that IMR technique might be a fully iterative reconstruction technique using various models. For example, accurate simulation of the Poisson distribution of the X-ray photon using a “statistical model” and the cone beam X-ray and the absorbing voxels using a “system physical model” were reported to suppress various artifacts [22]. High noise reduction rate of IMR might be well-suited for low-dose brain CT. Additionally, IMR offers a thin-slice volume acquisition with adequate image noise that allows multiplanar reconstruction (MPR). The clinical value of MPR images for brain disease in MRI has been widely reported [23, 24], and we consider that MPR brain CT images with IMR may be useful for improving the diagnostic performance of brain CT.

The development of unfamiliar texture with IMR was not a serious problem in the present study. However, it was previously reported that other full-IR techniques can exhibit a pixelated blotchy appearance and lack of familiarity for radiologists [25–27]. The cause of these contrasting results is unknown, although tuning of the reconstruction parameters of IMR to the brain may suppress this unfamiliar image texture. IMR changes the tuning of iterative reconstruction based on the body area and the experimental reconstructed images and thus may allow tuning of the IMR reconstruction parameters to mimic the conventional appearance of brain CT images with the FBP technique.

Another finding of our study was that FBP and HIR exhibited a similar CT number, while IMR exhibited a slightly lower CT number and higher contrast than other reconstruction technique. There is no phantom study about the change of the CT number at iterative model reconstruction for brain CT; therefore, a detailed phantom study may be required to define which reconstruction technique offers the most precise CT numbers. However, the increased contrast in IMR may be particularly suited to detection of slight attenuation changes in brain CT examination.

There are some limitations to our study. First, we did not evaluate the radiologist’s diagnostic performances for brain disease because the prevalence of brain disease in this study population is too low to perform such an evaluation. Large-scale clinical trials containing various patient cohorts are needed to evaluate the performance of IMR with low radiation dose brain CT. Second, we evaluated only one radiation dose setting in this study. Previous reports suggested that the other IR technique failed to improve the detectability of low-contrast objects at low radiation doses [19]. Additionally, there was only one phantom study about the IMR for brain CT in this study period [28]. Therefore, we cannot have confidence in the image quality of the IMR at extremely

low-dose setting and evaluated the innocuous dose setting for diagnosis in this study. Third, the small size of the sample may limit the generalization of our results. Finally, we used the DLP based on $CTDI_{vol}$ and the scan range to estimate the ED. Hurwitz et al. [29] reported that use of the DLP method to calculate ED could result in underestimations, compared with direct organ measurements. Therefore, we may have underestimated the ED in our study, as accurate ED evaluation requires direct organ measurements.

In conclusion, the IMR offers significant noise reduction and higher contrast and CNR in brain CT, especially with thin-slice images, when compared to FBP and HIR.

Compliance with ethical standards We declare that all human and animal studies have been approved by the Institutional Review Board and have therefore been performed in accordance with the ethical standards laid down in the 1964 Declaration of Helsinki and its later amendments. We declare that all patients gave informed consent prior to inclusion in this study.

Conflict of interest ST is an employee of Philips Electronics.

References

1. Sodickson A, Baeyens PF, Andriole KP, Prevedello LM, Nawfel RD, Hanson R et al (2009) Recurrent CT, cumulative radiation exposure, and associated radiation-induced cancer risks from CT of adults. *Radiology* 251:175–184
2. Berrington de Gonzalez A, Mahesh M, Kim KP, Bhargavan M, Lewis R, Mettler F et al (2009) Projected cancer risks from computed tomographic scans performed in the United States in 2007. *Arch Intern Med* 169:2071–2077
3. Brenner DJ, Hall EJ (2007) Computed tomography—an increasing source of radiation exposure. *N Engl J Med* 357:2277–2284
4. Barber PA, Demchuk AM, Zhang J, Buchan AM (2000) Validity and reliability of a quantitative computed tomography score in predicting outcome of hyperacute stroke before thrombolytic therapy. ASPECTS study group. *Alberta stroke programme early CT score. Lancet* 355:1670–1674
5. Hill MD, Demchuk AM, Tomsick TA, Palesch YY, Broderick JP (2006) Using the baseline CT scan to select acute stroke patients for IV-IA therapy. *AJNR Am J Neuroradiol* 27:1612–1616
6. Tamm EP, Rong XJ, Cody DD, Ernst RD, Fitzgerald NE, Kundra V (2011) Quality initiatives: CT radiation dose reduction: how to implement change without sacrificing diagnostic quality. *Radiographics* 31:1823–1832
7. Lee B, Newberg A (2005) Neuroimaging in traumatic brain imaging. *NeuroRx* 2:372–383
8. Joseph PM, Ruth C (1997) A method for simultaneous correction of spectrum hardening artifacts in CT images containing both bone and iodine. *Med Phys* 24:1629–1634
9. Doczi T, Schwarcz A (2003) Correlation of apparent diffusion coefficient and computed tomography density in acute ischemic stroke. *Stroke* 34:e17–18, author reply e17–18
10. Kucinski T, Vaterlein O, Glauche V, Fiehler J, Klotz E, Eckert B et al (2002) Correlation of apparent diffusion coefficient and computed tomography density in acute ischemic stroke. *Stroke* 33:1786–1791
11. Pickhardt PJ, Lubner MG, Kim DH, Tang J, Ruma JA, del Rio AM et al (2012) Abdominal CT with model-based iterative

- reconstruction (MBIR): initial results of a prospective trial comparing ultralow-dose with standard-dose imaging. *AJR Am J Roentgenol* 199:1266–1274
12. Katsura M, Matsuda I, Akahane M, Sato J, Akai H, Yasaka K et al (2012) Model-based iterative reconstruction technique for radiation dose reduction in chest CT: comparison with the adaptive statistical iterative reconstruction technique. *Eur Radiol* 22:1613–1623
 13. Chang W, Lee JM, Lee K, Yoon JH, Yu MH, Han JK et al (2013) Assessment of a model-based, iterative reconstruction algorithm (MBIR) regarding image quality and dose reduction in liver computed tomography. *Invest Radiol* 48:598–606
 14. Notohamiprodjo S, Deak Z, Meurer F, Maertz F, Mueck FG, Geyer LL et al (2015) Image quality of iterative reconstruction in cranial CT imaging: comparison of model-based iterative reconstruction (MBIR) and adaptive statistical iterative reconstruction (ASiR). *Eur Radiol* 25:140–146
 15. Machida H, Takeuchi H, Tanaka I, Fukui R, Shen Y, Ueno E et al (2013) Improved delineation of arteries in the posterior fossa of the brain by model-based iterative reconstruction in volume-rendered 3D CT angiography. *AJNR Am J Neuroradiol* 34:971–975
 16. Huda W, Ogden KM, Khorasani MR (2008) Converting dose-length product to effective dose at CT. *Radiology* 248:995–1003
 17. McCollough CH, Yu L, Kofler JM, Leng S, Zhang Y, Li Z et al (2015) Degradation of CT low-contrast spatial resolution due to the use of iterative reconstruction and reduced dose levels. *Radiology* 276:499–506
 18. Schindera ST, Odedra D, Raza SA, Kim TK, Jang HJ, Szucs-Farkas Z et al (2013) Iterative reconstruction algorithm for CT: can radiation dose be decreased while low-contrast detectability is preserved? *Radiology* 269:511–518
 19. Nishizawa M, Tanaka H, Watanabe Y, Kunitomi Y, Tsukabe A, Tomiyama N (2015) Model-based iterative reconstruction for detection of subtle hypoattenuation in early cerebral infarction: a phantom study. *Jpn J Radiol* 33:26–32
 20. Kijewski PK, Bjarngard BE (1978) Correction for beam hardening in computed tomography. *Med Phys* 5:209–214
 21. De Man B, Nuyts J, Dupont P, Marchal G, Suetens P (2001) An iterative maximum-likelihood polychromatic algorithm for CT. *IEEE Trans Med Imaging* 20:999–1008
 22. De Man B, Basu S (2004) Distance-driven projection and backprojection in three dimensions. *Phys Med Biol* 49:2463–2475
 23. Patzig M, Burke M, Bruckmann H, Fesl G (2014) Comparison of 3D cube FLAIR with 2D FLAIR for multiple sclerosis imaging at 3 tesla. *RöFo* 186:484–488
 24. Tanaka T, Morimoto Y, Shiiba S, Sakamoto E, Kito S, Matsufuji Y et al (2005) Utility of magnetic resonance cisternography using three-dimensional fast asymmetric spin-echo sequences with multiplanar reconstruction: the evaluation of sites of neurovascular compression of the trigeminal nerve. *Oral Surg Oral Med Oral Pathol Oral Radiol Endod* 100:215–225
 25. Deak Z, Grimm JM, Treitl M, Geyer LL, Linsenmaier U, Komer M et al (2013) Filtered back projection, adaptive statistical iterative reconstruction, and a model-based iterative reconstruction in abdominal CT: an experimental clinical study. *Radiology* 266:197–206
 26. Di Tommaso L, Destro A, Fabbris V, Spagnuolo G, Laura Fracanzani A, Fargion S et al (2011) Diagnostic accuracy of clathrin heavy chain staining in a marker panel for the diagnosis of small hepatocellular carcinoma. *Hepatology* 53:1549–1557
 27. Roger VL, Go AS, Lloyd-Jones DM, Benjamin EJ, Berry JD, Borden WB et al (2012) Executive summary: heart disease and stroke statistics—2012 update: a report from the American heart association. *Circulation* 125:188–197
 28. Love A, Olsson ML, Siemund R, Stalhammar F, Bjorkman-Burtscher IM, Soderberg M (2013) Six iterative reconstruction algorithms in brain CT: a phantom study on image quality at different radiation dose levels. *Br J Radiol* 86:20130388
 29. Hurwitz LM, Yoshizumi TT, Goodman PC, Frush DP, Nguyen G, Toncheva G et al (2007) Effective dose determination using an anthropomorphic phantom and metal oxide semiconductor field effect transistor technology for clinical adult body multidetector array computed tomography protocols. *J Comput Assist Tomogr* 31:544–549